PHYSICAL REVIEW B **79**, 081401(R) (2009)

Polarization fields in nitride-based quantum dots grown on nonpolar substrates

Stefan Schulz,[1] Arnaud Berube,[1] and Eoin P. O'Reilly[1,2]
[1]*Tyndall National Institute, Lee Maltings, Cork, Ireland*
[2]*Department of Physics, University College, Cork, Ireland*
(Received 2 December 2008; published 9 February 2009)

We use a surface-integral method to determine the polarization potential in nitride-based quantum dots (QDs) grown on a nonpolar substrate. There is uncertainty in the literature regarding the sign of the piezoelectric constant e_{15}. We find that only a negative e_{15} can give the reduced electrostatic built-in field found experimentally in nonpolar GaN/AlN QDs. Our analysis of nonpolar InN/GaN QDs indicates that a significant built-in field remains in these structures. We calculate that despite the reduced polarization potential, ground-state electrons and holes can remain spatially separated in GaN/AlN QDs.

DOI: 10.1103/PhysRevB.79.081401 PACS number(s): 68.65.Hb, 73.22.Dj, 77.22.Ej, 77.65.Ly

Nitride semiconductors are of great topical interest due to their potential applications in optoelectronic devices and high-power and/or high-temperature electronic devices.[1] The great majority of nitride-based quantum dots (QDs) with a wurtzite crystal structure are grown along the polar [0001] direction. A unique feature of these systems is the existence of large spontaneous and strain-induced polarizations, leading to a strong electrostatic field along the growth direction.[2] This leads to a spatial separation of electron and hole wave functions and consequent reduction in the radiative recombination rate.[3,4] To circumvent these problems, there has been a rapid increase in studies of nonpolar growth of III-nitride structures, where the [0001] direction lies in the growth plane.[5–8] Growth of quantum wells (QWs) along a nonpolar direction can eliminate polarization-induced fields, and hence give improved radiative recombination rates.[9]

We investigate here the effect of spontaneous and strain-induced polarization in QD structures grown on nonpolar substrates. It is not *a priori* obvious how the polarization potential should behave in such a QD. The built-in potential in a QW grown along the [0001] direction can be described in terms of induced charges due to the discontinuity in the polarization at the QW interface. When a QD is grown along a nonpolar direction, it still has [0001]-oriented side facets. The discontinuity in the polarization at these side facets, as well as the variation in strain through the dot, should then lead to a net polarization potential across the QD. Initial optical measurements suggest that the polarization potential is eliminated in nonpolar GaN/AlN QDs.[6,7] In this Rapid Communication we use a surface-integral method we have previously developed[10] to systematically investigate the electrostatic built-in field in nonpolar nitride-based QDs, comparing our results with those for polar *c*-plane QDs. There is uncertainty in the literature as to the sign of the piezoelectric constant e_{15} associated with shear strain.[11–14] We show that the built-in field in nonpolar GaN/AlN QDs is only significantly reduced if e_{15} is negative, while we predict for InN/GaN QDs that there should still be a significant field present, independent of the sign of e_{15}. In addition, we study the influence of the QD geometry on the built-in field, showing that the field is very sensitive to the actual geometry, with the built-in potential showing largest variation close to the [0001] facets of a nonpolar dot. We have also calculated the energies and wave functions of single-particle states in the framework of an effective-mass approximation. We find that it is possible to get an enhanced overlap between electron and hole states in nonpolar QDs, but that the overlap is sensitive to the dot geometry. We suggest that the large overlap observed in existing QD samples may in fact be due to overlap between ground-state electrons and excited-state holes.

The total built-in polarization $\mathbf{P}$ in a nitride-based nanostructure with a wurtzite crystal structure is given by $\mathbf{P}=\mathbf{P}^{\epsilon}+\mathbf{P}^{\mathrm{sp}}$. The first contribution, $\mathbf{P}^{\epsilon}$, is the strain-induced piezoelectric polarization, while the term $\mathbf{P}^{\mathrm{sp}}$ refers to the spontaneous polarization, due to the lack of inversion symmetry along the *c* axis of a wurtzite lattice. Self-assembled QDs typically have a large aspect ratio, with the ratio of dot base length *L* to dot height *H* as $\frac{L}{H}\sim 5-10$.[7,15] As a first approximation, the strain distribution in a dot is then similar to that in a QW of height *H*. We therefore begin our analysis by first comparing the total built-in polarizations $\mathbf{P}$ in a polar and a nonpolar QW structure.

Because of the crystal symmetry, the spontaneous polarization vector $\mathbf{P}^{\mathrm{sp}}$ is oriented along the *c* axis. The polarization potential ϕ_{sp} due to $\mathbf{P}^{\mathrm{sp}}$ in a polar QW structure then arises due to the difference at the QW interface, $\Delta\mathbf{P}^{\mathrm{sp}}=\mathbf{P}^{\mathrm{sp}}_{\mathrm{QW}}-\mathbf{P}^{\mathrm{sp}}_{\mathrm{B}}$, between the well and barrier spontaneous polarization vectors.

The second contribution to the built-in potential arises from $\mathbf{P}^{\epsilon}$, which depends on the local strain as[10]

$$\mathbf{P}^{\epsilon}=\begin{pmatrix} 2e_{15}\epsilon_{xz} \\ 2e_{15}\epsilon_{yz} \\ e_{31}(\epsilon_{xx}+\epsilon_{yy})+e_{33}\epsilon_{zz}\end{pmatrix}=\begin{pmatrix} P_{\mathrm{shear,x}} \\ P_{\mathrm{shear,y}} \\ P_{\mathrm{axial}}\end{pmatrix}, \qquad (1)$$

where e_{ij} denotes the different piezoelectric constants and ϵ_{ij} denotes the different strain components. For a QW grown along the *c* axis, there is no strain in the surrounding matrix material, and no shear strain in the QW, so that $\mathbf{P}^{\epsilon}$ also points along the *c* axis, and is of magnitude $P_{\mathrm{axial}}=I_{xy}+I_z$ in the well and zero outside, where $I_{xy}=e_{31}(\epsilon_{xx}+\epsilon_{yy})$ and $I_z=e_{33}\epsilon_{zz}$. There are then three terms which contribute to the total built-in potential, namely, the spontaneous term due to $\Delta\mathbf{P}^{\mathrm{sp}}$ plus two further terms due to I_{xy} and I_z.

In the case of a polar GaN/AlN QW structure, each of the

three terms is of the same sign, thereby all contributing to the large built-in field observed in such structures. The strain components ϵ_{xx} and ϵ_{yy} are given by $\epsilon_{xx}=\epsilon_{yy}=\frac{a_{\mathrm{AlN}}-a_{\mathrm{GaN}}}{a_{\mathrm{GaN}}}$, while $\epsilon_{zz}=\frac{-2C_{13}}{C_{33}}\epsilon_{xx}$, where C_{ij} are elastic constants and a_{AlN} and a_{GaN} are the lattice constants of AlN and GaN perpendicular to the c-axis. If not indicated otherwise, all parameters are taken from Ref. 16. In this polar QW case ϵ_{xx} and ϵ_{yy} are negative, while ϵ_{zz} is positive. Since e_{31} is negative and e_{33} is positive, we then have $I_{xy}=+0.026$ C/m^2 and $I_z=+0.012$ C/m^2. Finally, $\Delta\mathbf{P}^{\mathrm{sp}}$ is also positive, with $\Delta\mathbf{P}^{\mathrm{sp}}=+0.056$ C/m^2.

The situation for a QW grown along a nonpolar axis is different. We set the growth direction parallel to the x axis, with the y and z axes then in the growth plane. The in-plane strain components ϵ_{yy} and ϵ_{zz} are then given by $\epsilon_{yy}=\frac{1}{a_{\mathrm{GaN}}}(a_{\mathrm{AlN}}-a_{\mathrm{GaN}})$ and $\epsilon_{zz}=\frac{1}{c_{\mathrm{GaN}}}(c_{\mathrm{AlN}}-c_{\mathrm{GaN}})$, where c is the c-axis lattice constant, with $\epsilon_{xx}=-\frac{1}{C_{11}}(C_{12}\epsilon_{xx}+C_{13}\epsilon_{zz})$. In contrast to the c-plane system, ϵ_{zz} is now negative and ϵ_{xx} is positive, while ϵ_{yy} remains unchanged. For the nonpolar system I_z is then negative, with $I_z=-0.035$ C/m^2. The sign of the contribution I_{xy} depends on the sign of $(\epsilon_{xx}+\epsilon_{yy})$. Using the parameters of Ref. 16, $|\epsilon_{xx}|<|\epsilon_{yy}|$ and thus I_{xy} remains positive, but of reduced magnitude, with $I_{xy}=+0.002$ C/m^2. Therefore, the z component of the piezoelectric polarization will be reduced in a nonpolar QW compared to the conventional polar system. Because $\mathbf{P}^{\epsilon}$ is constant and there are no [0001] interfaces, there is no built-in potential within the nonpolar QW system. However, for a QD grown along a nonpolar direction, there will be a discontinuity in the polarization at the [0001] side facet interfaces. There will in addition be shear strain components ϵ_{xz} and ϵ_{yz} in and around the dot, and the magnitude of the axial strain components will vary through the dot. All of these factors will contribute to a net polarization potential across the dot.

To study in detail the polarization potential, we compare first cuboid polar and nonpolar GaN/AlN QDs of size $20\times18\times2$ nm^3. The potential due to $\mathbf{P}^{\mathrm{sp}}$ will depend on the polarization charge at the QD-barrier [0001] interfaces. Although the surface charge covers a smaller area in the nonpolar QD, the wider charge separation leads to nearly the same potential difference $\Delta\phi_{\mathrm{sp}}$ between the two QD-barrier interfaces for the polar and nonpolar cuboid QDs. This is confirmed by the spontaneous potential ϕ_{sp} (dashed green line) plotted in Fig. 1, along the c axis through the center of the dot for (a) a polar and (b) a nonpolar QD.

The situation is more complicated for the piezoelectric term $\mathbf{P}^{\epsilon}$, which depends on the strain state of the system. We calculate the piezoelectric contribution to the potential using the surface-integral method of Williams *et al.*,[10] which assumes isotropic material parameters. The P_{axial} contribution to the overall polarization potential, ϕ_{ax}, is shown by the solid blue diamond lines in Fig. 1. It can be seen that the magnitude of ϕ_{ax} is significantly reduced in the nonpolar case, as expected from the comparison of P_{axial} in polar and nonpolar QWs.

Turning to the shear strain component, there is a large degree of uncertainty in the shear piezoelectric constant ϵ_{15}.[17] In particular there is uncertainty not only in the magnitude of e_{15}, but also conflicting evidence as to its sign. For example, Refs. 11 and 12 report a positive value for e_{15}, while Refs. 13 and 14 find a negative sign.

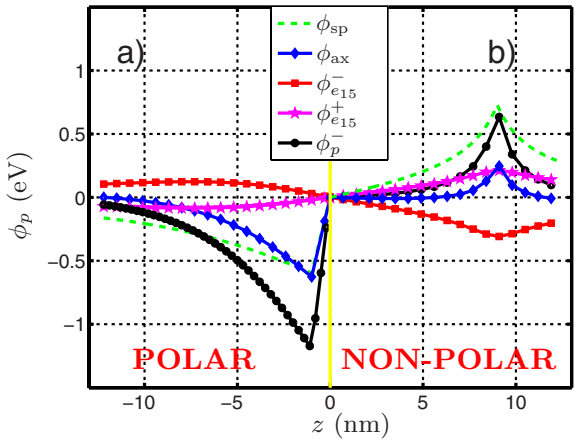

FIG. 1. (Color online) The different contributions to the total built-in potential ϕ_p for (a) polar and (b) nonpolar GaN/AlN QDs. The spontaneous polarization contribution is denoted by ϕ_{sp}. The different components of piezoelectric potential are given by ϕ_{ax} and ϕ_{15}. The index $\pm$ indicates the sign of the piezoelectric constant e_{15}. The total piezoelectric potential ϕ_p^- (black solid line) assumes a negative e_{15}.

To investigate the contribution of e_{15} and the terms P_{shear} in Eq. (1) to the electrostatic potential, we first use the e_{15} value of Ref. 10, which is positive ($e_{15}=0.33$ C/m^2). The resulting $\phi^+_{e_{15}}$ is shown by the purple line with stars in Fig. 1 for (a) the polar and (b) the nonpolar QDs. We see for the polar QD that the shear strain contribution $\phi^+_{e_{15}}$ is small compared to the axial contribution ϕ_{ax}. For the nonpolar case, $\phi^+_{e_{15}}$ exceeds the axial part ϕ_{ax} through much of the dot. Furthermore, with e_{15} positive, these two contributions would both add to the spontaneous contribution to give a large total polarization potential. Using a negative value for e_{15}, e.g., $e_{15}=-0.48$ C/m^2,[17] the contribution $\phi^-_{e_{15}}$ is again small compared to the axial part ϕ_{ax} in the c-plane QD structure [cf. red line with squares in Fig. 1(a)]. For the nonpolar QD, ϕ^-_{15} is again of larger magnitude than ϕ_{ax} through much of the dot, but this time is of opposite sign [red square line in Fig. 1(b)]. Therefore, the shear strain contribution $\phi^-_{e_{15}}$ approximately cancels both the axial part ϕ_{ax} and also much of the spontaneous part ϕ_{sp} in the center of the dot. We calculate that the potential difference $\Delta\phi$ between the two facets is then reduced by a factor of order 2 in the nonpolar QD, compared to the potential difference in the polar case. In addition, most of the potential drop occurs close to the side facets in the nonpolar QD, whereas the potential varies approximately linearly between the top and bottom surfaces of the polar QD.

In practice, QDs do not have vertical sidewall such as considered in Fig. 1. The atomic force microscopy (AFM) analysis of a-plane GaN/AlN QDs (Ref. 7) shows that these nanostructures form as truncated pyramids with a mean diameter of 20 nm and a height of 2 nm. Similar dimensions are found in Refs. 5 and 6. Recent experimental results[8] reveal that the studied a-plane GaN/AlN QDs have a nonsquare shape, with the in-plane dimension slightly larger

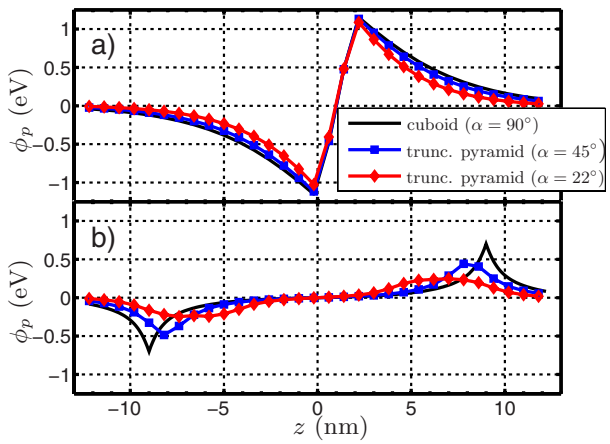

FIG. 2. (Color online) The electrostatic potential ϕ_p for (a) c- and (b) a-plane QDs as a function of angle α of the QD facets.

along the $[1\bar{1}00]$ than along the [0001] direction. Therefore, we assume a truncated pyramid with a rectangular base of 20×18 nm^2 and a height of 2 nm. The in-plane dimension ratio is then 0.9, comparable to the experimentally observed one of (0.89 ± 0.14).[8] For comparison, the same geometry is used for the c-plane QDs. We consider three truncated pyramids, with different sidewall angles α of 90°, 45°, and 22°, where α denotes the angle between the QD facet and the c axis in the nonpolar dot (α=90° for a cuboid dot). We see from Fig. 1 how the potential reaches a maximum on a c-plane facet, dropping in magnitude on both sides of the facet. The maximum built-in potential change will therefore be reduced with sloping facets because the sidewalls are distributed over a range of z values. Figures 2(a) and 2(b) show the variation in potential along the c axis through the center of the dot for the polar and the nonpolar systems, respectively. As expected, the potential ϕ_p of the c-plane QD is almost unaffected by the change in α. By contrast, the peak electrostatic potential decreases with decreasing sidewall angle α in the nonpolar case. We suggest that a detailed study of the shape of these structures is now required to evaluate accurately the likely scale of the built-in potential in nonpolar QDs.

To gain insight on the influence of the electrostatic built-in field, we calculate the electron- and hole-confined single-particle states using an effective-mass approximation. The model includes different effective masses for the holes along different directions. In a conventional c-plane system the first two valence-band states have essentially p_x- and p_y-like orbital characters ($|X\pm iY\rangle$), with p_z character removed from the valence-band edge due both to the crystal-field splitting and to strain.[18] For c-plane dots, we therefore use the effective hole masses given in Ref. 19. In a nonpolar QD, strain lifts the symmetry in the xy plane. This leads to a separation of the $|X\pm iY\rangle$-like states. The energy of the $|Y\rangle$ state is raised, while that of the $|X\rangle$ state is lowered due to strain, with $|Z\rangle$ calculated to be again below $|Y\rangle$ due to the crystal-field splitting and confining effects. The effective hole masses along the x, y, and z directions for the highest valence band are then given in the diagonal approximation by $m_h^{-1}=m_0^{-1}(A_2+A_4+A_5,A_2+A_4-A_5,A_1+A_3)$, where m_0 is the bare electron mass. The highest hole band then has a light-hole mass along the y direction, and a heavy mass in the xz plane. The parameters A_i, the effective electron mass, and the band offsets are taken from Ref. 16. For a more complete description of the single-particle states, multiband methods, such as a $\mathbf{k}\cdot\mathbf{p}$ (Ref. 20) or tight-binding approach,[4] are required to take band-mixing effects into account. However, we are interested here in insights into the physics of nonpolar nitride-based QDs rather than a full description of all aspects of these QDs. Therefore, the effective-mass approximation should be sufficient to identify the influence of the electrostatic built-in field on the localized electron and hole wave functions.[21] The resulting electron $|\psi_1^e|^2$ and hole $|\psi_1^h|^2$ ground-state probability density of the truncated pyramidal c-plane GaN/AlN QD is shown in Fig. 3(a). The angle α is chosen to be α=22°. The corresponding probability densities for the nonpolar system are shown in Fig. 3(b). Even though the electrostatic built-in potential is strongly reduced in the nonpolar QD, a clear spatial separation of electron and hole ground-state probability densities is observed. This effect can be attributed to the large dimension along the [0001] direction. This result is confirmed by comparing the calculated modulus squared overlap $d_{11}=|\langle\psi_1^e|\psi_1^h\rangle|^2$ of electron and hole ground-state wave functions. In the case of the polar system we find $d_{11}^{\mathrm{p}}=0.36$, while in the nonpolar system we obtain $d_{11}^{\mathrm{np}}=0.16$; i.e., the electron-hole overlap is reduced because the hole wave function is largely confined by the electrostatic potential close to the [0001] facet. According to the tight-binding results of Ref. 22, the emission of c-plane nitride-based QDs is dominated by so-called skew excitons, which are excitons consisting of s-shell electrons and p-shell holes and vice versa. Therefore, we have also included in our analysis the overlap of the electron ground state ψ_1^e with the first excited hole state ψ_2^h. The corresponding probability densities are shown in Fig. 3(c) for the polar system and in Fig. 3(d) for the nonpolar system. In the case of the polar system, the electron ground state and the first excited hole state are orthogonal. This is in contrast to the result we find in the nonpolar system. Here, we observe that the electron ground-state probability density $|\psi_1^e|^2$ strongly overlaps with the probability density $|\psi_2^h|^2$ of the first excited hole state. Again, these results are confirmed by looking at d_{12} of the electron and hole wave functions. For the polar system we find $d_{12}^{\mathrm{p}}=0$, while the nonpolar structure yields $d_{12}^{\mathrm{np}}=0.38$. The ground-state overlap calculated here differs markedly from the values deduced from the experimental analysis in Ref. 6, where a large overlap has been deduced from photoluminescence measurements. We suggest that further investigation is now required to reconcile the difference between the predicted and measured overlaps, to identify whether skew excitons are being measured experimentally and/or whether the built-in field in a nonpolar QD is smaller than that predicted here.

In addition to GaN/AlN QDs, InN/GaN QDs are of technological interest. The principal difference between c-plane GaN/AlN QDs and InN/GaN QDs is the relative contribution of spontaneous and piezoelectric potentials to the total potential. While the potential of GaN/AlN QDs is nearly evenly distributed between the two sources, the InN/GaN QDs are

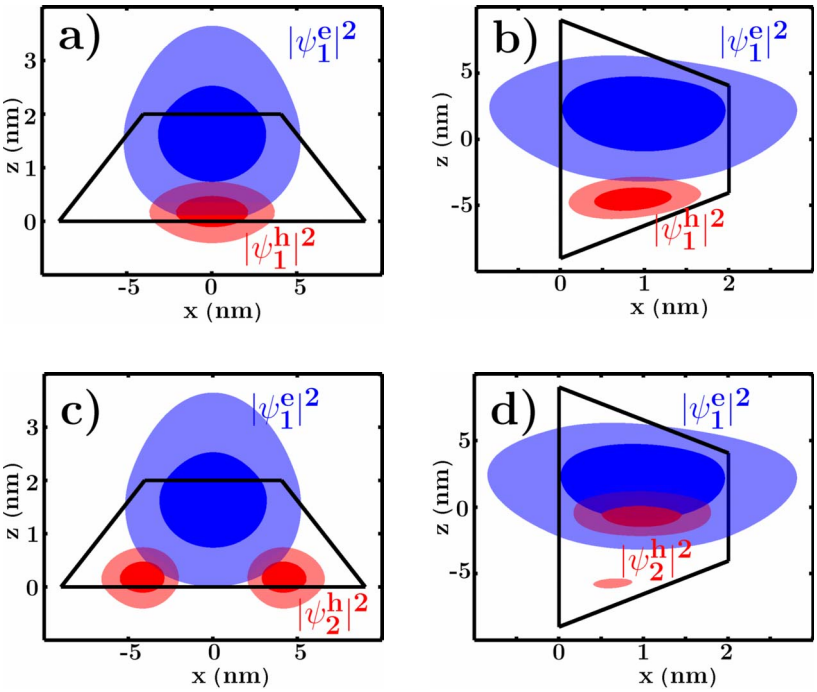

FIG. 3. (Color online) Side view of the model QD geometry for polar and nonpolar systems, showing isosurfaces of the probability densities for electrons (blue/dark gray) and holes (red/gray) at 50% (light) and 80% (dark) of the maximum value. For the polar QD the electron $|\psi_1^e|^2$ and hole $|\psi_1^h|^2$ ground-state probability density is shown in (a), while (c) shows the probability density of the electron ground state and the first excited state $|\psi_2^h|$. The corresponding results for the nonpolar QD are shown in (b) and (d), respectively.

dominated by the piezoelectric potential.[10] We see in Fig. 1 that the low field through the center of a GaN/AlN nonpolar QD arises due to cancellation of significant spontaneous and strain-induced polarization contributions to the potential. Further calculations we have undertaken show that there will therefore be a much stronger potential variation ($\geq \sim 0.1$ eV nm^{-1}) across an InN/GaN QD of similar dimensions to the GaN/AlN dot considered in Fig. 1. Therefore, it is expected that the electrostatic built-in field will still lead to a spatial separation of electron and hole wave functions, even when e_{15} is negative.

In conclusion we have analyzed the different contributions to the electrostatic potential in nonpolar wurtzite QDs. Our investigations reveal that only a negative value of e_{15} can give a strong reduction in the built-in field in nonpolar GaN/AlN QDs, as observed experimentally. Because the contribution from the spontaneous polarization is negligible in InN/GaN QDs compared to the strain-induced component, a significant electrostatic built-in field is then expected even in nonpolar systems. We find that the built-in potential is strongly sensitive to the dot shape, decreasing when the QD side facets are at an angle to the *c* plane. Despite the reduced built-in potential, we find that the overlap of the electron and hole ground-state wave functions can be even smaller than that found in comparable *c*-plane QDs. Further investigation is now required to confirm the role of the built-in polarization potential in nonpolar wurtzite QDs.

This work was supported by Science Foundation Ireland (SFI). S.S. acknowledges further support from the Humboldt Foundation. A.B. was supported by an SFI UREKA Site Grant No. UR/06/1916.

[1] S. C. Jain *et al.*, J. Appl. Phys. **87**, 965 (2000).
[2] J. Simon, N. T. Pelekanos, C. Adelmann, E. Martinez-Guerrero, R. Andre, B. Daudin, L. S. Dang, and H. Mariette, Phys. Rev. B **68**, 035312 (2003).
[3] A. D. Andreev and E. P. O'Reilly, Appl. Phys. Lett. **79**, 521 (2001).
[4] S. Schulz, S. Schumacher, and G. Czycholl, Phys. Rev. B **73**, 245327 (2006).
[5] N. Garro *et al.*, Appl. Phys. Lett. **87**, 011101 (2005).
[6] S. Founta *et al.*, Appl. Phys. Lett. **86**, 171901 (2005).
[7] S. Founta *et al.*, Phys. Status Solidi B **243**, 3968 (2006).
[8] S. Founta *et al.*, J. Appl. Phys. **101**, 063541 (2007).
[9] P. Waltereit *et al.*, Nature (London) **406**, 865 (2000).
[10] D. P. Williams, A. D. Andreev, E. P. OReilly, and D. A. Faux, Phys. Rev. B **72**, 235318 (2005).
[11] S. Muensit, E. M. Goldys, and I. L. Guy, Appl. Phys. Lett. **75**, 3965 (1999).
[12] F. Bernardini and V. Fiorentini, Appl. Phys. Lett. **80**, 4145 (2002).
[13] K. Tsubouchi and M. Mikoshiba, IEEE Trans. Sonics Ultrason. **32**, 634 (1985).
[14] G. Bu *et al.*, Appl. Phys. Lett. **84**, 4611 (2004).
[15] N. T. Pelekanos *et al.*, J. Phys.: Conf. Ser. **10**, 61 (2005).
[16] I. Vurgaftman and J. R. Meyer, J. Appl. Phys. **94**, 3675 (2003).
[17] D. P. Williams, A. D. Andreev, and E. P. OReilly, Phys. Rev. B **73**, 241301(R) (2006).
[18] S. Schulz, S. Schumacher, and G. Czycholl, Eur. Phys. J. B **64**, 51 (2008).
[19] S. L. Chuang and C. S. Chang, Phys. Rev. B **54**, 2491 (1996).
[20] A. D. Andreev and E. P. O'Reilly, Phys. Rev. B **62**, 15851 (2000).
[21] J. A. Barker and E. P. O'Reilly, Phys. Rev. B **61**, 13840 (2000).
[22] N. Baer, S. Schulz, P. Gartner, S. Schumacher, G. Czycholl, and F. Jahnke, Phys. Rev. B **76**, 075310 (2007).